Available online at www.sciencedirect.com
SCIENCE DIRECT®
Journal of Photochemistry and Photobiology A: Chemistry 157 (2003) 167–184
Journal of Photochemistry and Photobiology A:Chemistry
www.elsevier.com/locate/jphotochem

Measurements of molecular absorption spectra with the SCIAMACHY pre-flight model: instrument characterization and reference data for atmospheric remote-sensing in the 230–2380 nm region

K. Bogumil, J. Orphal*, T. Homann, S. Voigt, P. Spietz, O.C. Fleischmann, A. Vogel, M. Hartmann, H. Kromminga, H. Bovensmann, J. Frerick, J.P. Burrows

Institute of Environmental Physics, University of Bremen, P.O. Box 33 04 40, 28334 Bremen, Germany

Received 27 June 2002; received in revised form 7 January 2003; accepted 16 January 2003

Abstract

Using the scanning imaging absorption spectrometer for atmospheric chartography (SCIAMACHY) pre-flight model satellite spectrometer, gas-phase absorption spectra of the most important atmospheric trace gases (O_3, NO_2, SO_2, O_2, OClO, H_2CO, H_2O, CO, CO_2, CH_4, and N_2O) have been measured in the 230–2380 nm range at medium spectral resolution and at several temperatures between 203 and 293 K. The spectra show high signal-to-noise ratio (between 200 up to a few thousands), high baseline stability (better than 10^{-2}) and an accurate wavelength calibration (better than 0.01 nm) and were scaled to absolute absorption cross-sections using previously published data. The results are important as reference data for atmospheric remote-sensing and physical chemistry. Amongst other results, the first measurements of the Wulf bands of O_3 up to their origin above 1000 nm were made at five different temperatures between 203 and 293 K, the first UV-Vis absorption cross-sections of NO_2 in gas-phase equilibrium at 203 K were recorded, and the ultraviolet absorption cross-sections of SO_2 were measured at five different temperatures between 203 and 296 K. In addition, the molecular absorption spectra were used to improve the wavelength calibration of the SCIAMACHY spectrometer and to characterize the instrumental line shape (ILS) and straylight properties of the instrument. It is demonstrated that laboratory measurements of molecular trace gas absorption spectra prior to launch are important for satellite instrument characterization and to validate and improve the spectroscopic database.

Keywords: SCIAMACHY; Absorption spectra; Trace gases; Remote-sensing

1. Introduction

The observation of the changing atmosphere requires powerful observational techniques that enable global monitoring of atmospheric trace gas concentrations with high spatial resolution. For this purpose, a new generation of optical remote-sensing instruments for monitoring of atmospheric trace gases from space has been developed in the last decade (ca. 1990–2000). These satellite instruments operate in the ultraviolet, visible and near-infrared regions of the spectrum and use backscattered and surface- or cloud-reflected sunlight to detect several important atmospheric constituents such as O_3, NO_2, SO_2, H_2CO, OClO, BrO, and H_2O using their characteristic absorption features in the UV-Vis region. Amongst the most powerful instruments is the scanning imaging absorption spectrometer for atmospheric chartography (SCIAMACHY) spectrometer [1,2] that was launched into orbit (800 km) in early 2002 on-board the European ENVISAT-1 satellite. SCIAMACHY uses two scanning mirrors, one for Nadir- and one for Limb-scanning of the atmosphere, and eight dedicated measurements channels between 230 and 2380 nm, using highly sensitive diode-array detectors with 1024 pixel elements each. Its optical bench is temperature-stabilized to better than 0.1 K, and it uses the sun and on-board light sources and additional polarization measurement devices for spectral and radiometric calibration.

The detection of O_3, NO_2 and other atmospheric trace gases by means of absorption spectroscopy requires accurate knowledge of their absorption cross-sections at all relevant atmospheric temperatures and pressures. Using the SCIAMACHY proto-flight model (PFM) spectrometer a new data set of temperature-dependent absorption cross-sections was measured in 1998–2000 prior to the integration of SCIAMACHY on the ENVISAT platform in 2001. The new data

* Corresponding author. Present address: Laboratoire de Photophysique Moléculaire, CNRS, Bât. 350, Centre d'Orsay, 91405 Orsay Cedex, France. Tel.: +33-1-6915-752886; fax: +33-1-6915-753055.
E-mail address: johannes.orphal@ppm.u-psud.fr (J. Orphal).

1010-6030/03/$ – see front matter © 2003 Elsevier Science B.V. All rights reserved.
doi:10.1016/S1010-6030(03)00062-5

set comprises absorption cross-sections of O_3, NO_2, SO_2, O_2, OClO, H_2CO, H_2O, CO, CO_2, CH_4, and N_2O measured over the whole spectral range of the SCIAMACHY spectrometer (230–2380 nm) and in a broad temperature range (203–293 K). The absorption cross-sections will be included in the SCIAMACHY data processing for the retrieval of column densities and vertical distributions of atmospheric trace gases from the satellite measurements. In order to obtain absorption cross-sections at intermediate temperatures if necessary a temperature parametrization is applied to the O_3, NO_2 and SO_2 absorption cross-sections. The molecular absorption cross-sections were also used for improving the wavelength calibration of the SCIAMACHY spectrometer and for characterizing the instrumental line shape (ILS) and the straylight properties of the instrument.

2. Experimental set-up

2.1. The SCIAMACHY spectrometer

The SCIAMACHY spectrometer is a multi-channel grating spectrometer operating in the ultraviolet, visible and near infrared wavelength regions at medium resolution (see Table 1). It measures continuously between 230 and 1760 nm with a spectral resolution of 0.24–1.48 nm (full-width at half-maximum (FWHM) of the instrumental line shape, ILS) and in two additional spectral windows between 1940–2040 and 2265–2380 nm (spectral resolution of 0.22 and 0.26 nm, respectively). A double spectrometer design with a pre-disperser prism and gratings in the eight channels is used to cover this large wavelength range and to suppress straylight inside the spectrometer. The light is detected by cooled diode arrays detectors with 1024 pixels consisting of silicon for wavelengths below 1000 nm and of InGaAs for the near infrared wavelength region. The pixel exposure times can independently be chosen for each channel. The spectrometer shows high stability and can measure very small absorptions due to its high dynamic range. A CrPt/Ne-hollow cathode emission lamp (calibrated by interferometric measurements before the instrument integration) and a broad-band white light source (quartz/tungsten/halogen lamp) are available on-board for spectral and radiometric calibration and instrument monitoring during flight. A more detailed description of the SCIAMACHY instrument is given in [1,2], see also Section 7.

Table 1
Parameters of the spectral channels of the SCIAMACHY instrument

Channel	Spectral range in nm	Spectral resolution in nm
1	240–314	0.24
2	309–405	0.26
3	394–620	0.44
4	604–805	0.48
5	785–1050	0.54
6	1000–1750	1.48
7	1940–2040	0.22
8	2265–2380	0.26

During the measurements of the absorption cross-sections the SCIAMACHY spectrometer was controlled by a dedicated on-ground electronics (EGSE) developed and operated by Dornier-Astrium, Germany, the instrument being cooled down to operational temperatures (the temperature of the optical bench and detector modules being monitored and maintained constant to better than 0.1 K) and operated inside of a high vacuum tank at Fokker Space (Schiphol, The Netherlands). Therefore, all wavelengths mentioned in this paper are given for vacuum conditions, and are extremely stable (better than 0.01 nm) due to the active temperature stabilization of the SCIAMACHY optical bench. Prior to the measurements presented in this paper the SCIAMACHY spectrometer was characterized and calibrated by industry (consortium of Fokker Space, Dornier-Astrium, TPD–TNO, SRON and others) providing data concerning the pixel-to-pixel gain, stray light properties, the instrumental line shape in each channel, the wavelength calibration and the polarization properties [3].

2.2. The CATGAS set-up

Calibration apparatus for trace gas absorption spectra (CATGAS) is a transportable set-up for absorption spectroscopy consisting of two coolable quartz glass cells, different light sources and a gas system for static and flow gas measurements. It may be operated at temperatures (180–350 K) and pressures (0.1–1000 mbar) relevant to the stratosphere and troposphere. The main components of CATGAS are two double jacketed quartz glass cells (volume ca. 3000 cm^3). The inner jacket of the cells are floated by a circulating cooling fluid (ethanol), while the outer jackets are evacuated for thermal isolation. For this purpose, the cells are additionally wrapped by an isolating foam. The cooling fluid is pumped through the inner jackets by a two-stage cryocooler (Haake KT90) for the one cell and a cooling thermostat (Haake F6-C40) for the other cell. For the measurements described in this paper, temperatures between 293 and 203 K were adjusted in the cells, with an absolute accuracy of better than ±1 K (using a pre-cooler for flow experiments at the lowest temperatures), calibrated before the measurements using a Pt100 temperature element in the cell. Both cells contain a White optics [4] with a base path of 120 cm and a *f*-number of 60. Optical paths of 505 and 985 cm were used for the measurements described here (there is an additional path of each 12.5 cm before and after the White optics, leading to the numbers given above). Using two cells greatly facilitates the work at different temperatures since one of the slowest processes is cooling down these cells to low temperatures.

The light of either a Xenon-lamp (ILC Technology, 300 W) for the ultraviolet and visible wavelength region or a quartz/tungsten/halogen lamp (Osram, 250 W) for the visible and near infrared wavelength region is focused into

Table 2
Experimental conditions for the measured gases and number of different partial pressures measured for each absorber

Gas	Spectral range in nm	SCIAMACHY channels	Temperatures in K	No. of different partial pressures
O_3	230–1075	1–6	293, 273, 243, 223, 203	5
NO_2	230–930 (293 K), 233–890 (273, 243 K), 233–769 (223 K), 241–760 (203 K)	1–5	293, 273, 243, 223, 203	2–4 (depending on temperature)
SO_2	239–395	1–2	293, 273, 243, 223, 203	2
OClO	290.5–460	1–3	293	1
H_2CO	247.3–400	1–2	293	1
O_2	235–389 (293 K), 235–440 (243 K), 650–799.6 (293, 243 K), 235–330 (203 K), 650–787 (203 K)	1, 4	293, 243, 203	1
H_2O	1940–2040	7	293	2
CO_2	1945–1980, 1995–2032	7	293, 243	2–4
CO	2300–2380	8	293, 243	2–3
N_2O	2265–2300	8	293, 243	1–2
CH_4	2265–2380	8	293, 243	2–4

one of the cells using an off-axis parabolic mirror, a spherical and a flip mirror. After having passed the cell the light is focused on the entrance of a quartz glass fibre bundle (diameter 6.2 mm) consisting of about 8000 single fibres (75% UV-enhanced and 25% IR-enhanced) made by Schott, Germany. The other end of the fibre bundle is formed as a slit and imaged on the entrance slit of the SCIAMACHY spectrometer so that the slit is fully and homogeneously illuminated. Note however that the aperture of the fibres (about 20°) is much larger than the field-of-view of the SCIAMACHY instrument leading to loss of photons. The imaging optics however was far away from the entrance slit of the spectrometer and no additional straylight was produced. For wavelength calibration using an external source the light of a CrPtNe hollow cathode emission lamp (LOT Oriel) was focused on the entrance of the glass fibre bundle.

Table 2 gives an overview of the trace gases and experimental conditions. Measurements were performed using either gas mixtures flowing through the cell or static conditions. Absorption measurements in a gas flow were used for gases which are photolyzed by the analyzing light in order to maintain a constant column density in the cell. The cells were flushed with different gas mixtures maintained stable using calibrated gas flow controllers (MKS). The following mixtures were used: NO_2, NO or SO_2 in N_2; pure O_2; O_3 in a mixture of O_2 and N_2; and OClO in a mixture of O_3, O_2 and N_2. The NO_2, NO and SO_2 were taken from commercial gas bottles (Messer Griesheim) with a certified mixture of 1% NO_2, NO or SO_2 in N_2. These mixtures were additionally diluted with nitrogen (N_2 5.0) as carrier gas. The O_3 was generated by flowing oxygen (O_2 5.0) through a commercial ozonizer (Innovatec OG5) containing a silent discharge. The oxygen was also used for the measurements of pure oxygen.

The concentrations of each trace gas were carefully adjusted to match the different absorptions of the gases in different wavelength regions, and to avoid saturation effects (this was validated before the SCIAMACHY measurements using dedicated measurements at the IUP, Bremen, Germany). After mixing the gases were cooled by passing through a cold container (pre-cooler) adjusted to the same temperature as the CATGAS cells prior to entering the absorption volume. The pressure in the cells was permanently monitored by two capacitive manometers (MKS Baratron). The total pressures varied between 50 and 900 mbar for different measurements. After flushing through the cells the ozone was destroyed by a hot platinum wire, all other gases except N_2 and O_2 were trapped by a cryogenic trap.

For the static measurements another gas system was used, which was separated from the flow system by valves. The cells were filled with static gas mixtures of CO, CO_2, N_2O or CH_4 in N_2 prepared in a gas mixing system (two large balloons made of Pyrex) at a total pressure of 500 mbar in the cell and at different partial pressures of the trace gases. H_2O was filled into the cell at its saturated vapour pressure. Most interestingly very rapid aerosol formation was observed even at pressures below the H_2O saturated vapour pressure leading to strong scattering in the UV and visible channels. For H_2CO a reduced pressure was used in order to avoid saturation effects. The H_2CO photolysis by the analysis light was negligibly small over the time used for recording the spectra described here (a few minutes), probably due to the low UV output of our light source.

2.3. Measurement procedure

For each temperature and gas mixture the following measurement procedure was applied: First the pixel exposure times in the different channels were optimized for the selected combination of light source, cell and pathlength. Then a shutter after the end of the fibre bundle was closed and the dark current was measured for the chosen pixel exposure times.

Thereafter a spectrum of the lamp was recorded without any absorber in the cell. During this measurement the cell

only filled with the carrier gas (N_2). After evacuation the cell was filled with the gas mixture to be measured. After having achieved equilibrium conditions in the cell an absorption spectrum was recorded and the gas mixture was pumped out of the cell. At last a lamp spectrum was again measured in order to monitor lamp drifts. Each measurement took 320 s, while the detectors of the different channels were repeatedly read out.

At the beginning and end of each day a spectrum of the CrPtNe lamp either on CATGAS or built in the SCIAMACHY spectrometer was recorded for wavelength calibration. Once a week a spectrum of the internal white light source in the SCIAMACHY spectrometer was measured.

Three measurement series were performed with the SCIAMACHY pre-flight model. In October 1998 the so-called "PI-Period" took place. After modifications of the instrument the "Delta-PI-Period" (January 1999) and the "Delta2-PI-Period" (January 2000) were performed. During the latter two campaigns, only measurements in channels concerned by the instrument modifications were repeated. The total measurement time was about 5 weeks.

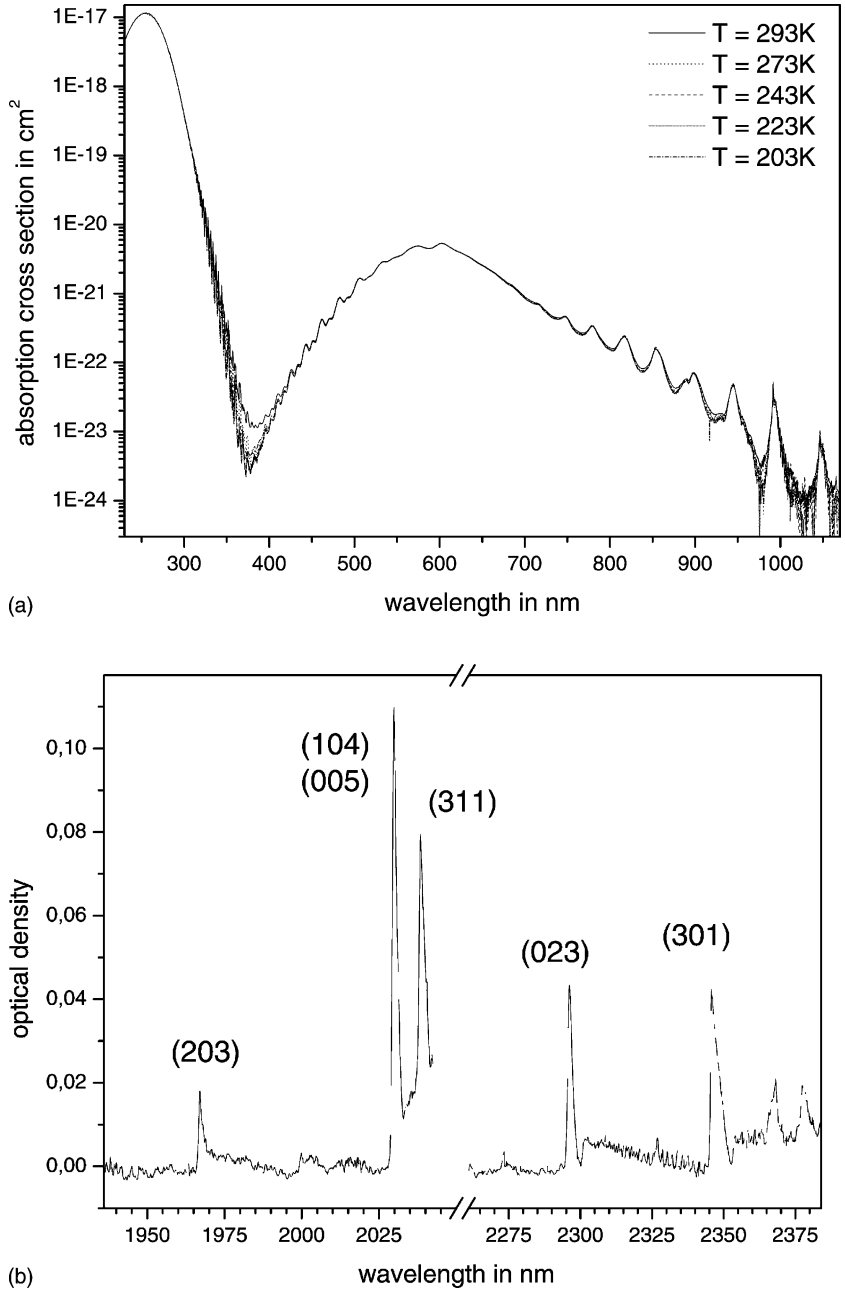

Fig. 1. O_3 absorption spectra measured with SCIAMACHY. (a) Absorption cross-sections of O_3 between 230 and 1070 nm at different temperatures. (b) Optical densities of O_3 at 293 K in the SCIAMACHY channels 7 and 8.

3. Data reduction and error budget

After inspection, the readouts of all individual channels were averaged for each channel, and for each measurement the dark current was subtracted from the two lamp spectra and the absorption spectrum. Then the uniform and the non-uniform ("ghost") spectral straylight was calculated for each spectrum employing a procedure defined during the calibration phase, i.e. using scaling factors for the uniform straylight in the different channels and polynomial coefficients describing the positions and intensities of the different spectral ghosts (see the more detailed description provided by industry [3]). For channel 1, a special straylight algorithm was applied due to the strong polarization dependence of the straylight in this channel [5]. The calculated straylight was subtracted from the lamp and from the absorption spectra. By dividing the lamp spectra measured before and after the absorption spectrum through each other, a possible lamp drift during the measurement and the signal-to-noise ratio was monitored. Usually the lamp drift was less than 1% and the signal-to-noise ratio was larger than 200 and in many cases up to a few 1000 (depending on wavelength

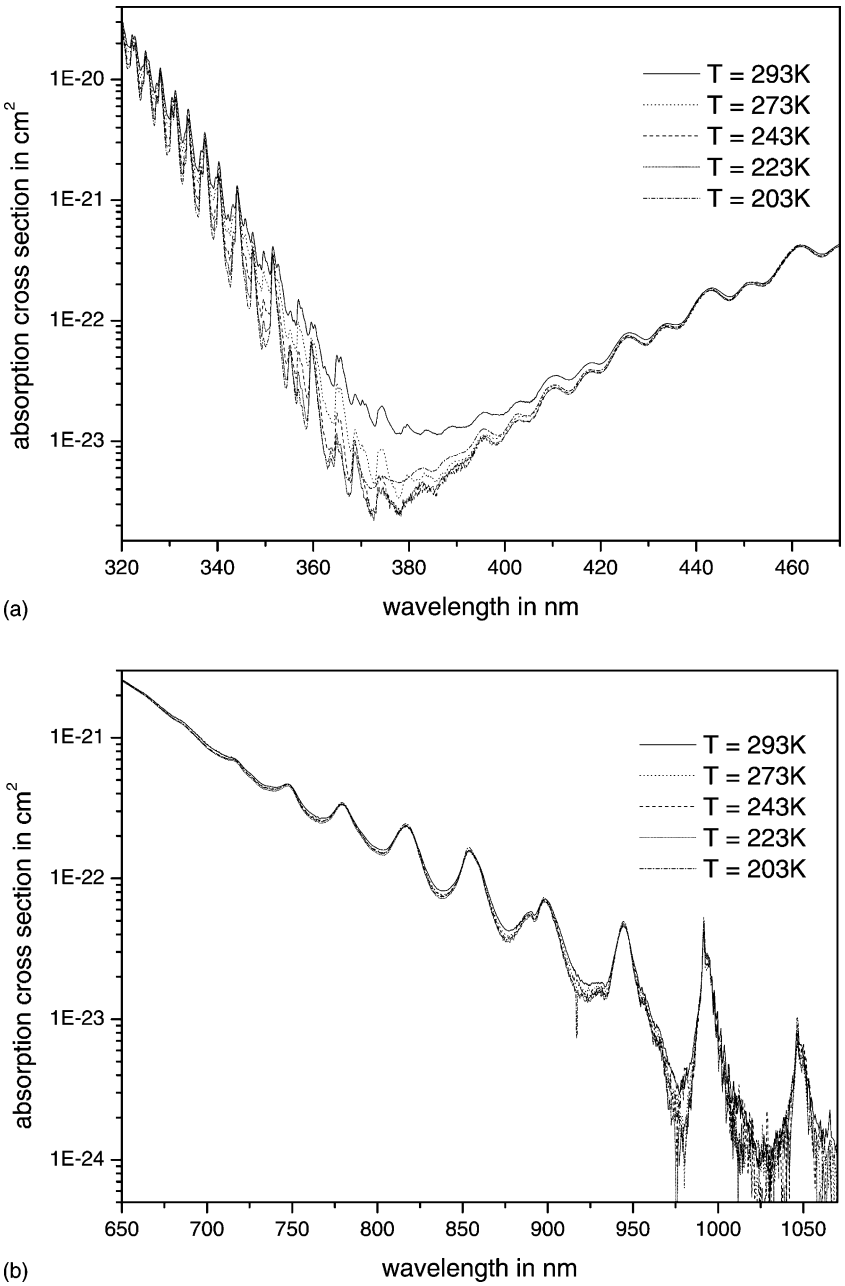

Fig. 2. O_3 absorption spectra measured with SCIAMACHY. (a) Absorption cross-sections of O_3 in the Huggins and Chappuis bands at different temperatures. (b) Absorption cross-sections of O_3 in the Wulf bands at different temperatures.

and the absorbers). The lamp spectra with the smaller drift in relation to the absorption spectrum and with the better signal-to-noise ratio was chosen as reference spectrum. At any rate the lamp spectrum with the higher signal-to-noise ratio was used. If both lamp spectra were of the same quality, they were weighted and averaged to obtain the reference spectrum. Then the optical density was calculated using the Beer–Lambert law.

If necessary the optical densities were corrected for residual lamp drifts by adding a constant value assuming the lamp drift was linear with time. The O_3 spectrum at 293 K had to be corrected for an additional OClO absorption, and the O_3 spectra at the other temperatures for some atomic lines in the Chappuis bands caused by the lights in the hall where the measurements took place. The spectra of NO_2 at 243, 223 and 203 K also comprised absorption of N_2O_4, which is formed in thermal equilibrium with NO_2 at low temperatures. They had to be corrected for this absorption by a procedure using three different optical densities of NO_2/N_2O_4 and based on the fact that N_2O_4 has negligible absorption at wavelengths above 400 nm [6,7]. For each molecule, the optical densities measured at different partial pressures were scaled to each other and were wavelength-calibrated using a fifth-order polynomial (as recommended by industry and

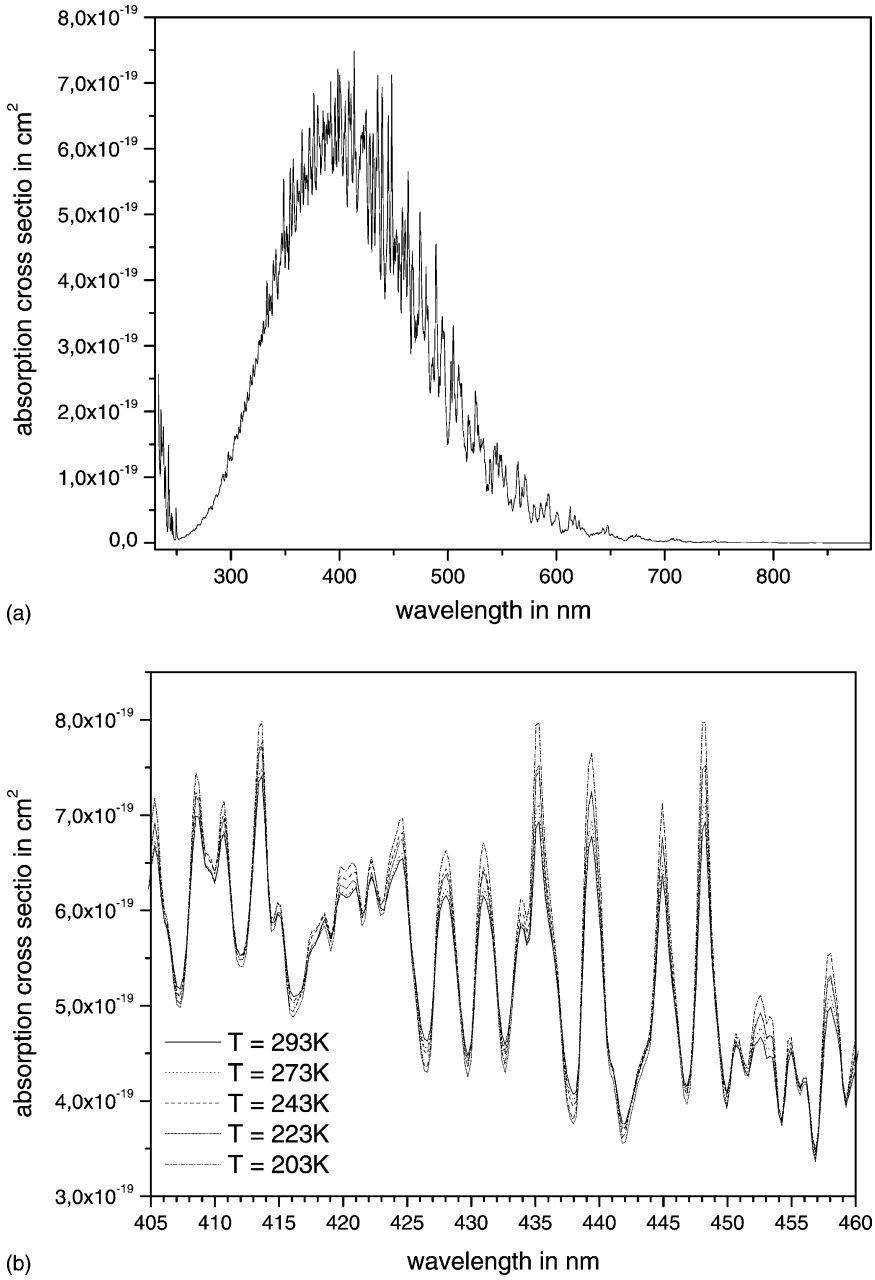

Fig. 3. NO_2 absorption spectra measured with SCIAMACHY. (a) Absorption cross-sections of NO_2 at 273 K. Note the very low noise as visible above 750 nm. (b) Absorption cross-sections of NO_2 in the 405–460 nm range at different temperatures.

by the SCIAMACHY Science Advisory Group during the calibration phase). Then the optical densities were concatenated to obtain complete spectra over the whole absorption wavelength range of the measured molecule. The overall uncertainty of the optical densities caused by lamp drifts and noise is always less than 1.1%.

In order to calculate absolute absorption cross-sections from the optical densities, the optical pathlength l and the partial pressure of the trace gas in the cell have to be known very precisely. Due to the limited time avaible during the PI periods the partial pressures of the trace gases could not be determined exactly. For this reason the optical densities were scaled to absolute absorption cross-sections using molecular absorption cross-sections from literature. The O_3 optical densities were scaled to absorption cross-sections calculated with the polynomial coefficients given by Bass and Paur [8]. The NO_2 and the SO_2 optical densities at 293 K were scaled to the absorption cross-sections measured by Vandaele et al. [9,10]. The optical densities at the other temperatures were scaled using the integrated absorption cross-section of the electronic transition, which is independent of temperature assuming that the electronic transition moment is independent from the nuclear coordinates in the temperature range 200–300 K [7,11,12]. The OClO optical density was scaled

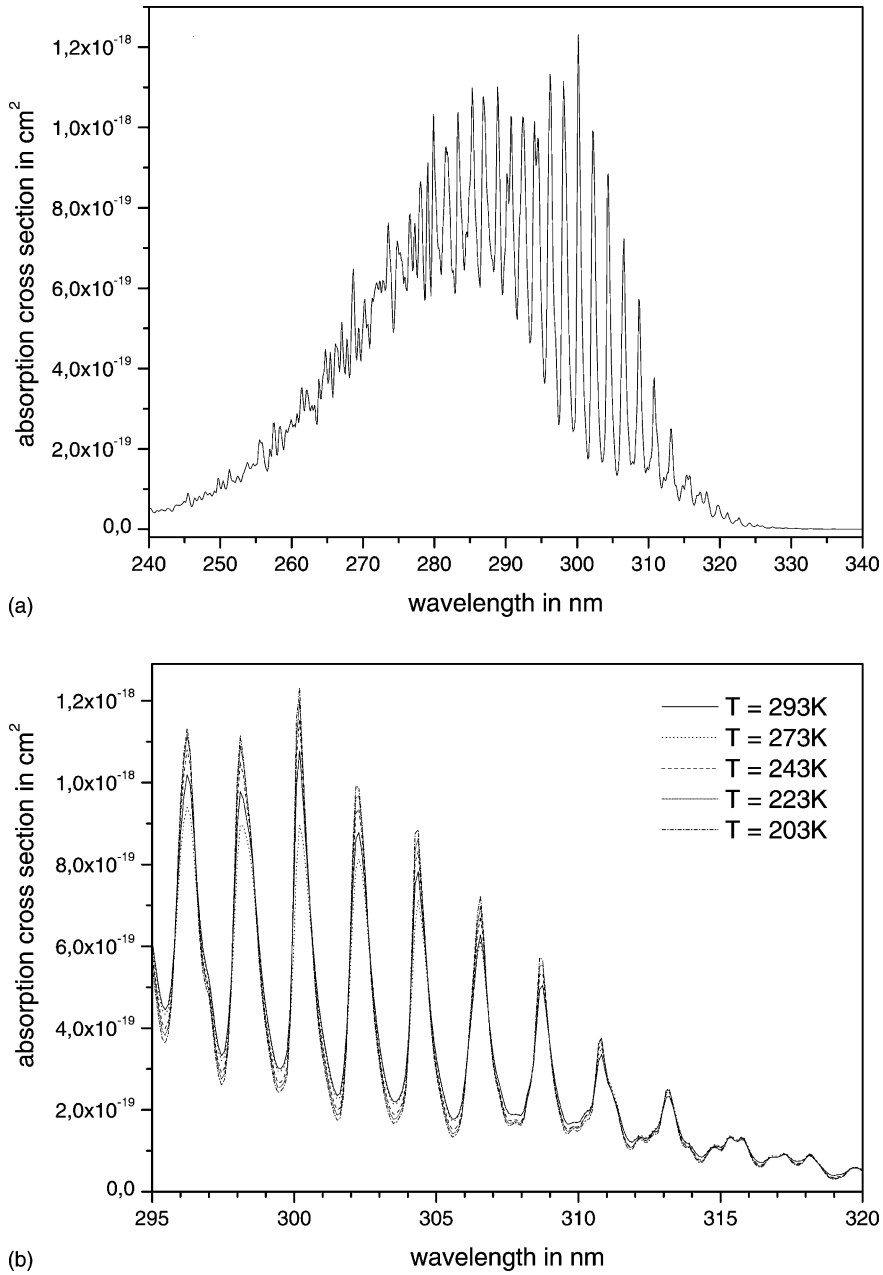

Fig. 4. SO_2 absorption spectra measured with SCIAMACHY. (a) Absorption cross-sections of SO_2 at 203 K. Note the very low noise as visible above 330 nm. (b) Absorption cross-sections of SO_2 in the 295–320 nm range at different temperatures.

to the absorption cross-sections measured by Kromminga et al. [13] and the O_2 optical densities were scaled using HITRAN data [14]. Further details of the concatenating and scaling procedures including detailed comparisons with previously published cross-sections are reported by Bogumil [15].

The uncertainty of the absorption cross-sections is given by the uncertainty of the optical densities, the uncertainty of the absorption cross-sections used for scaling, and the uncertainty in the scaling procedure, and is both dependent on statistical and systematic errors. Note that an accurate assessment of the error budget is a difficult task, which might be the reason for under-estimation of experimental errors in the past (see for example the comparisons made in [12]). In this work, the errors were obtained by summing up all error estimates using the square-root sum of the quadratic errors only for the statistical errors. A detailed description of these calculations is given by Bogumil [15].

In summary, the uncertainty of the O_3 absorption cross-sections is always 3.1% or less except for regions with cross-sections below 10^{-23} cm^2 and in the overlap region between channels 1 and 2 (305–320 nm) where the contribution

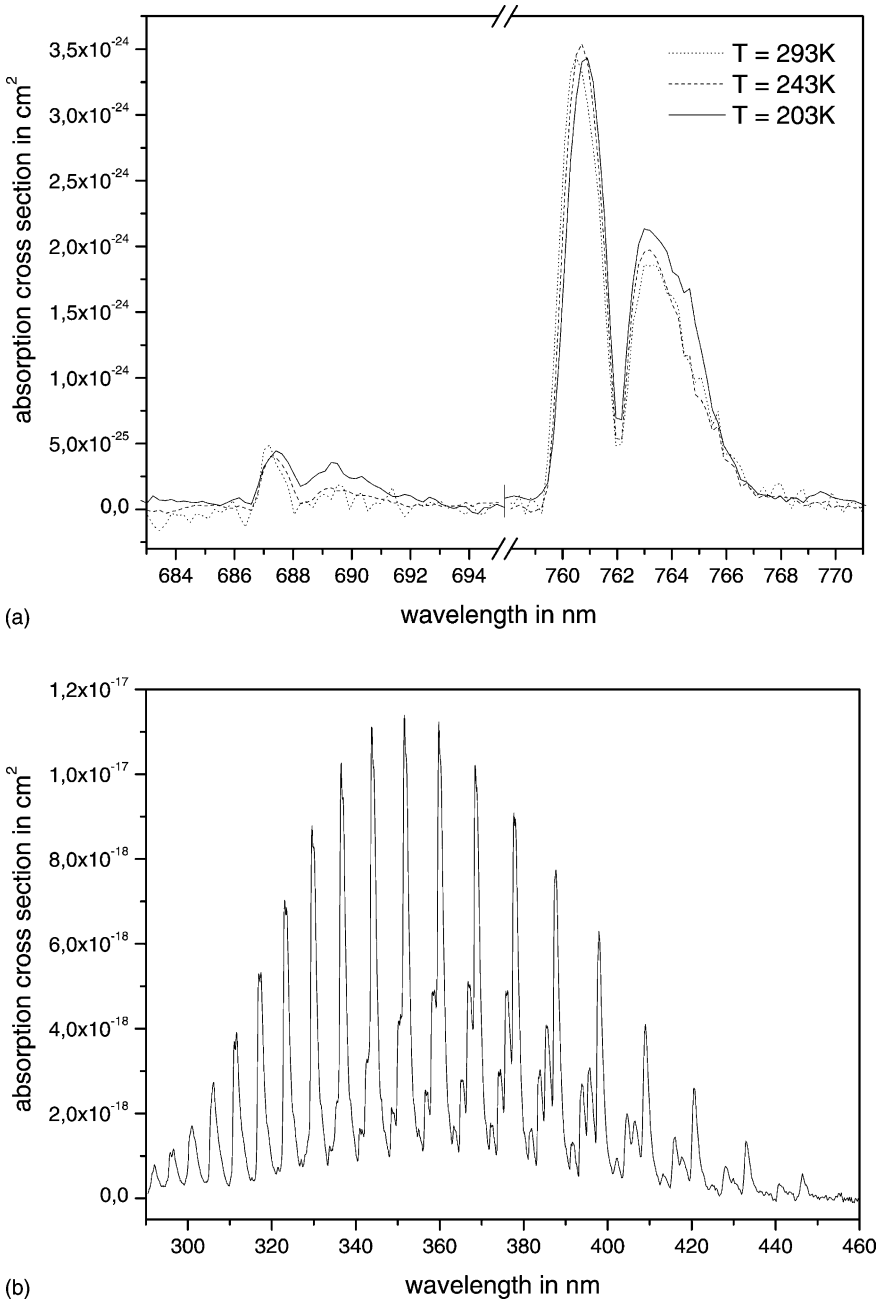

Fig. 5. O_2 and OClO absorption spectra measured with SCIAMACHY. (a) Absorption cross-sections of O_2 in the visible region at different temperatures. (b) Absorption cross-sections of OClO at 293 K.

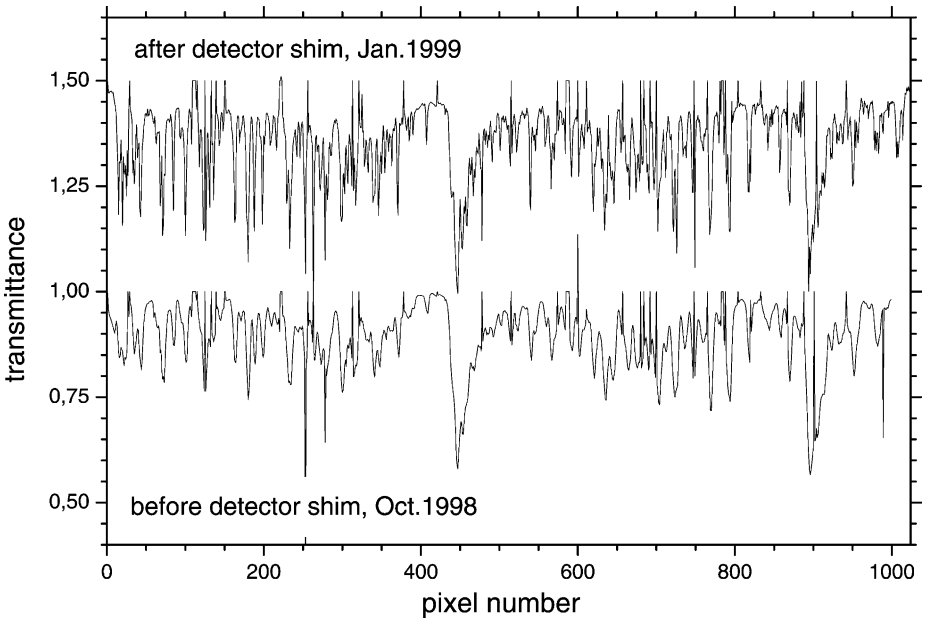

Fig. 6. Measured absorption spectra of CH_4 in SCIAMACHY channel 7. "Hot" and "bad" pixels are visible and have not been corrected for in this plot. Both spectra are shown over pixel numbers. Note that the detector shim has led to a spectral shift, too. The total pressure is 500 mbar to avoid saturated absorption of the spectral lines.

of uncorrected straylight is significant. The uncertainty of the NO_2 and SO_2 absorption cross-sections depends on the temperature and is 3.2% for the NO_2 absorption cross-sections at 293 K, 3.4% for the NO_2 absorption cross-sections at lower temperatures, 2.8% for the SO_2 absorption cross-sections at 293 K, and 3.0% for the SO_2 absorption cross-sections at lower temperatures. The overall uncertainty of the OClO absorption cross-sections is 8.5%. Note that for gases with highly structured spectra (OClO, NO_2, the near-infrared absorbers) that are much narrower than the SCIAMACHY ILS, the cross-sections contain an additional systematic error from the convolution which is difficult to assess and depends also strongly on the accuracy of the ILS determination. However for NO_2 and OClO the comparison with previously published data shows excellent agreement with less than 2% RMS deviations between the SCIAMACHY PFM spectra of this study and those recorded with high-resolution FTS [12,13].

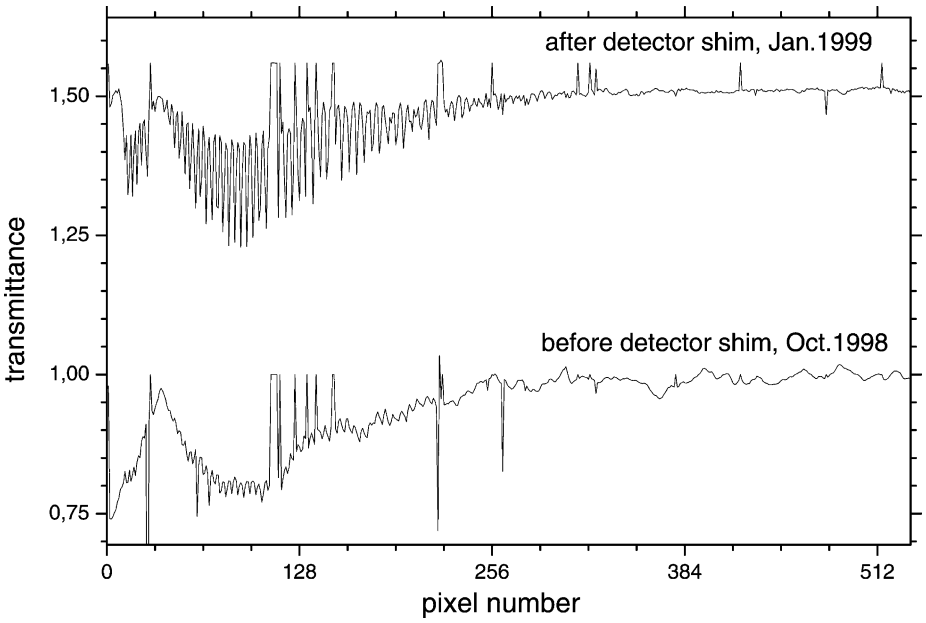

Fig. 7. Measured absorption spectra of N_2O in SCIAMACHY channel 8. "Hot" and "bad" pixels are visible and have not been corrected for in this plot. Both spectra are shown over pixel numbers. Note that the detector shim has led to a spectral shift, too.

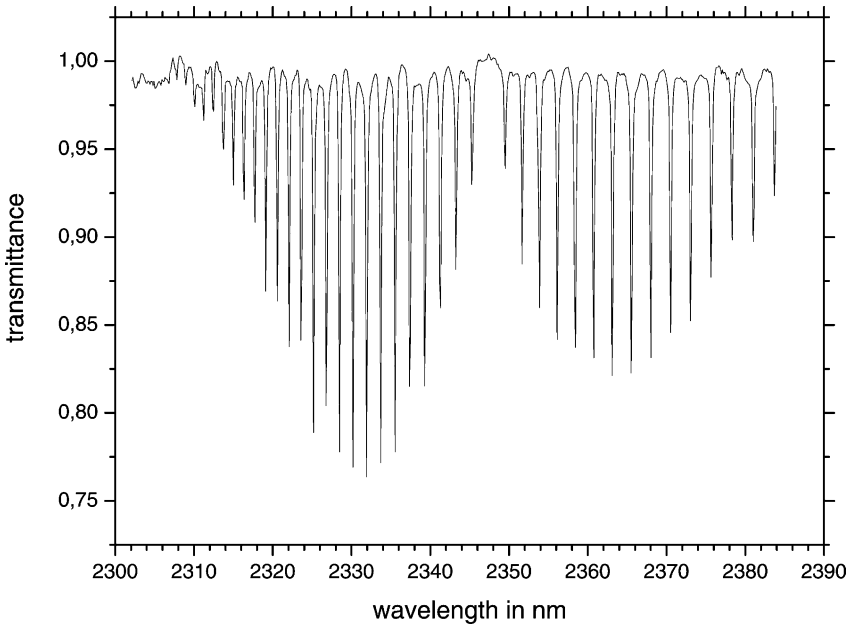

Fig. 8. Measured absorption spectrum of CO in SCIAMACHY channel 8.

4. Absorption cross-sections

In this section the measured temperature-dependent absorption cross-sections are presented. The absorption cross-sections vary with temperature because the rotational and vibrational state distribution in the electronic ground state changes with temperature. Generally the differential cross-sections increase with decreasing temperature.

Temperature-dependent absorption cross-sections of ozone were obtained from 230 to 1070 nm thus containing the band origin of the Wulf bands at 9553.13 cm^{-1} [16] (see Fig. 1a). In channels 7 and 8 the absorption to highly excited vibrational states can be observed (see Fig. 1b). The line positions and intensities of these bands have been measured recently by high-resolution Fourier-transform spectroscopy [17–21]. The temperature dependence of the Hartley, Huggins and Chappuis bands in the O_3 absorption cross-section is in agreement with previous studies [11,12,22–25]. Due to the high partial pressures of O_3 used in the measurements (up to about 100 mbar) and due

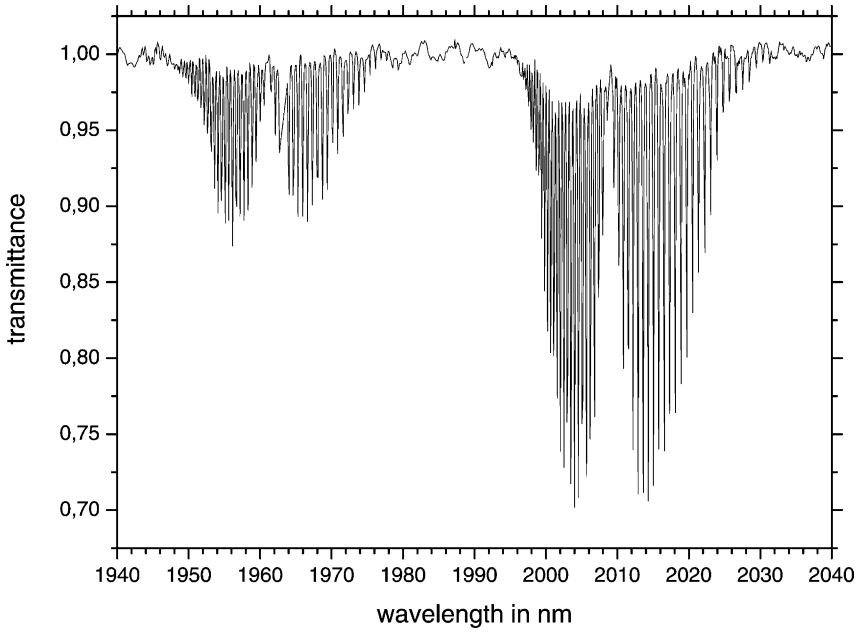

Fig. 9. Measured absorption spectrum of CO_2 in SCIAMACHY channel 7. Note the presence of small etalons in the baseline, probably from the CATGAS set-up.

to the high sensitivity of the SCIAMACHY spectrometer (noise-equivalent absorbance of about 10^{-4}), even the very weak absorption (about 10^{-23} cm^2 per molecule) between 350 and 420 nm was measured with a good signal-to-noise ratio of about 100 (see Fig. 2a). In the region above 900 nm one can see that the noise becomes visible at cross-sections of 10^{-24} cm^2 per molecule and below where the optical densities come close to the noise.

The hot and cold bands in the Huggins bands are clearly visible in these spectra. The intensity of the hot bands, arising from excited vibrational states in the electronic ground state, decreases with decreasing temperature, while the intensity of the cold band increases. With decreasing temperature the envelopes of the Huggins and the Chappuis bands move slightly towards shorter wavelengths (due to the change in the Franck–Condon points following from the depopulation of excited rotational–vibrational states in the electronic ground state with decreasing temperature) and the absorption between these two bands decreases. It is however unexplained why this absorption seems to increase again between 223 and 203 K. This was already observed in the ozone absorption cross-sections measured with the GOME FM spectrometer [11] and by Fourier-transform spectroscopy [7,25], so an error caused by lamp drifts is improbable, although systematic errors are not entirely excluded. Due to the high purity of the used gases, absorption of gaseous impurities is not to be expected. Maybe a weakly bound complex of O_3 and O_2 is formed at lower temperatures, as already proposed previously [25].

The temperature dependence of the Wulf bands was measured for the first time at more than two temperatures and over a broad spectral range (see Fig. 2b). In this region the differential absorption cross-sections vary by 20% between 293 and 203 K in the absorption peaks, probably due to the changing rotational population of the ground state. Note that one can even see part of the rotational fine structure of the band at 1000 nm, in agreement with very high-resolution work [16]. This region is also important because the oxygen A-band around 762 nm is used for cloud detection and determination of cloud properties, where the atmospheric O_3 absorption has to be taken into account [26].

Absorption cross-sections of NO_2 were measured between 203 and 293 K (see Fig. 3). The temperature dependence in the wavelength region used for atmospheric detection is shown in Fig. 3b. The absorption cross-sections measured by the SCIAMACHY spectrometer are compared with absorption cross-sections measured by the GOME spectrometer over a similar spectral range (231–794 nm) and at similar temperatures (221–293 K) [27]. The absorption cross-section measured by the GOME spectrometer are smaller at all temperatures than the SCIAMACHY absorption cross-sections (probably due to a different scaling reference, see reference [12]) but except for these differences the absorption cross-sections agree very well over a broad wavelength range. This shows that both sets of temperature-dependent absorption cross-sections do not contain residual N_2O_4 absorption and errors caused by lamp drifts.

In Fig. 4 the absorption cross-sections of SO_2 and their temperature dependence in the 295–320 nm wavelength range are shown. At 293 K the absolute absorption cross-sections agree within 5% with the absorption cross-sections measured by Vandaele et al. [10] and by Hearn and Joens [28], whereas the differential cross-sections measured by the SCIAMACHY spectrometer are slightly larger. The absorption cross-sections of O_2 and OClO are

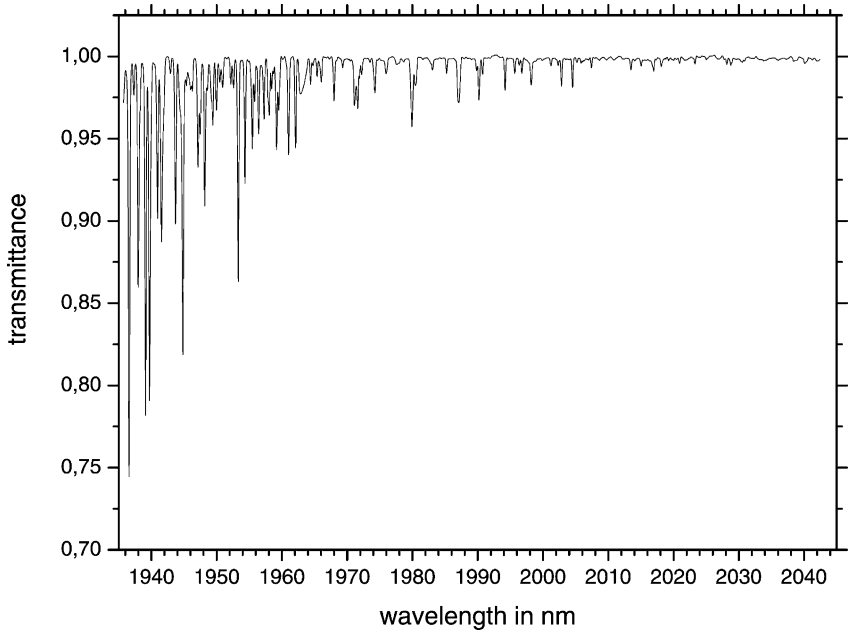

Fig. 10. Measured absorption spectrum of H_2O in SCIAMACHY channel 7.

presented in Fig. 5. The OClO absorption cross-sections were scaled to the absorption cross-sections measured by Kromminga et al. [12] and are therefore about 10% smaller than the absorption cross-sections measured by Wahner et al. [29]. The relative agreement between the SCIAMACHY cross-sections and those of Kromminga et al. [12] is indeed excellent, as shown in the latter paper. In addition to the data shown here, a spectrum of H_2CO at room temperature was recorded (with a signal-to-noise ratio of about 10^3) and also a few spectra of the radicals BrO and IO at different temperatures using Br or I atoms (produced by a silent discharge) mixed with gaseous O_3 and O_2.

5. Near-infrared absorbers

In order to validate the available spectroscopic database and to verify the instrumental line shape and spectral calibration parameters provided by industry [3], measurements of the most relevant atmospheric absorbers in the near-infrared

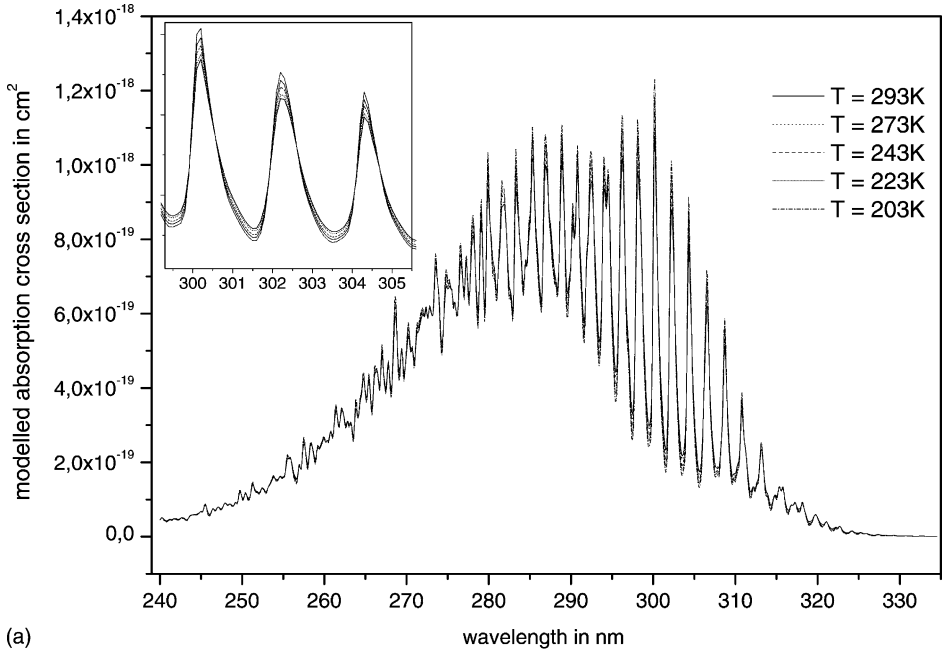

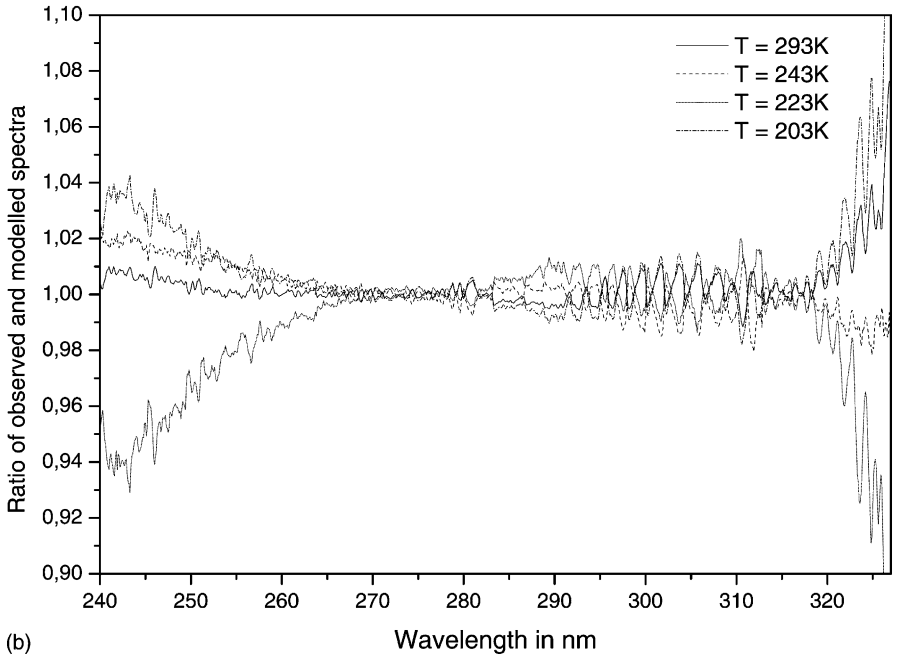

Fig. 11. SO_2 absorption spectra at different temperatures from a parametric model. (a) Modelled absorption cross-section of SO_2. (b) Ratio of the modelled and measured absorption cross-section of SO_2.

were also performed with the SCIAMACHY PFM: these are H_2O, CO_2, CO, N_2O and CH_4. Most of these gases were also measured at two different temperatures (see Table 2). Note that these measurements were extremely important in the identification of a serious problem with the near-infrared detector optics, since the detector arrays of channels 7 and 8 were slightly out of focus leading to a significant loss of resolution and thus of sensitivity towards differential absorption structures. Therefore, the SCIAMACHY instrument was refurbished in late 1998 (detector shim) and new trace gas measurements were undertaken in early 1999. There is a clear improvement in spectral resolution in the channels 7 and 8 (see Figs. 6 and 7). Examples of absorption spectra of CO, CO_2 and H_2O measured with the SCIAMACHY PFM after the refurbishment are presented in the Figs. 8–10. Note that this refurbishment was a crucial step in order to achieve the required sensitivity for measurements of atmospheric CO and N_2O from space. Comparisons of the measured spectra with the HITRAN database are currently in progress.

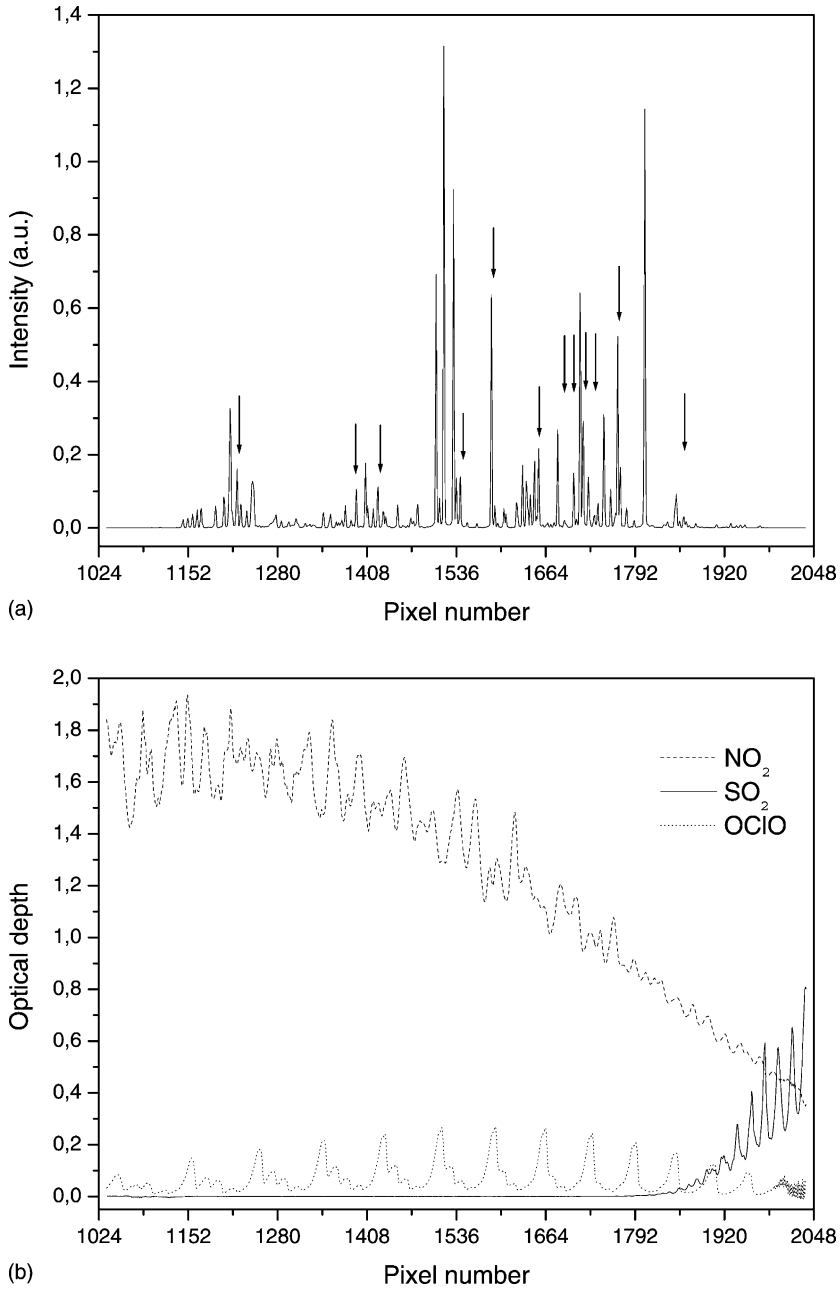

Fig. 12. Spectral calibration of the SCIAMACHY instrument. (a) Spectral lines of the CrPtNe hollow cathode lamp in channel 2 (309–405 nm). The spectral lines used for calibration are indicated by arrows. Note that the higher wavelengths are on the left side of the spectrum due to the readout order in channel 2. (b) Optical densities of OClO, NO_2 and SO_2 in channel 2 (309–405 nm) that were used for wavelength calibration. Note that the higher wavelengths are on the left side of the spectrum due to the readout order in channel 2.

6. Temperature parametrization of the absorption cross-sections

Absorption cross-sections are usually measured at selected temperatures. In order to characterize their temperature dependence and to calculate absorption cross-sections at intermediate temperatures, an empirical temperature parametrization is applied to the measured absorption cross-sections, using the following formula:

$$\sigma(\lambda, T) = \sigma(\lambda, T_0) \exp\left(-c_1(\lambda)\, T + \frac{c_2(\lambda)}{T}\right)$$

Note that for O_3 a quadratic formula is also very well adapted for the reproducing the temperature dependence of the absorption cross-sections within experimental uncertainties [8,12] and that for NO_2 and OClO a linear model with only two terms is sufficient [12,13]. However, the theoretical interpretation of the parameters needs further investigation.

In this way, noise in the spectra as well as small systematic errors due to lamp drifts and to unrecognised stray-light are significantly reduced. For example, for the SO_2 absorption cross-sections, this procedure was applied to describe the temperature dependence at each wavelength, the wavelength-dependent parameters being adjusted by a non-linear least-squares fitting routine in the wavelength range between 260 and 335 nm. The absorption spectrum at 273 K was however excluded because of problems caused by lamp drifts. For this temperature it is recommended to use only the modelled spectrum. The agreement between the measured and the modelled spectra is better than 2% between 260 and 320 nm (see Fig. 11). For smaller wavelengths, larger deviations are observed as a result of lamp drifts, and for longer wavelengths the deviations result from the small absorbances. The temperature parametrization was applied to the NO_2 absorption cross-sections in the 400–600 nm wavelength region and to the O_3 absorption cross-sections in the 320–350 nm wavelength region. The modelled spectra agree better than 2% with the measured spectra within these wavelength regions. The wavelength-dependent parameters can be obtained from the authors upon request.

7. SCIAMACHY instrument characterization

7.1. Wavelength calibration

The wavelength calibration of the SCIAMACHY spectrometer is performed using the spectral lines of an external CrPtNe lamp [3]. These lines were previously wavelength-calibrated using high-resolution Fourier-transform spectroscopy in the UV-Vis [30] and infrared [31] regions. However, the spectral lines are not evenly spread over the spectral range of the SCIAMACHY instrument (see Fig. 12a). Especially at the borders of the channels

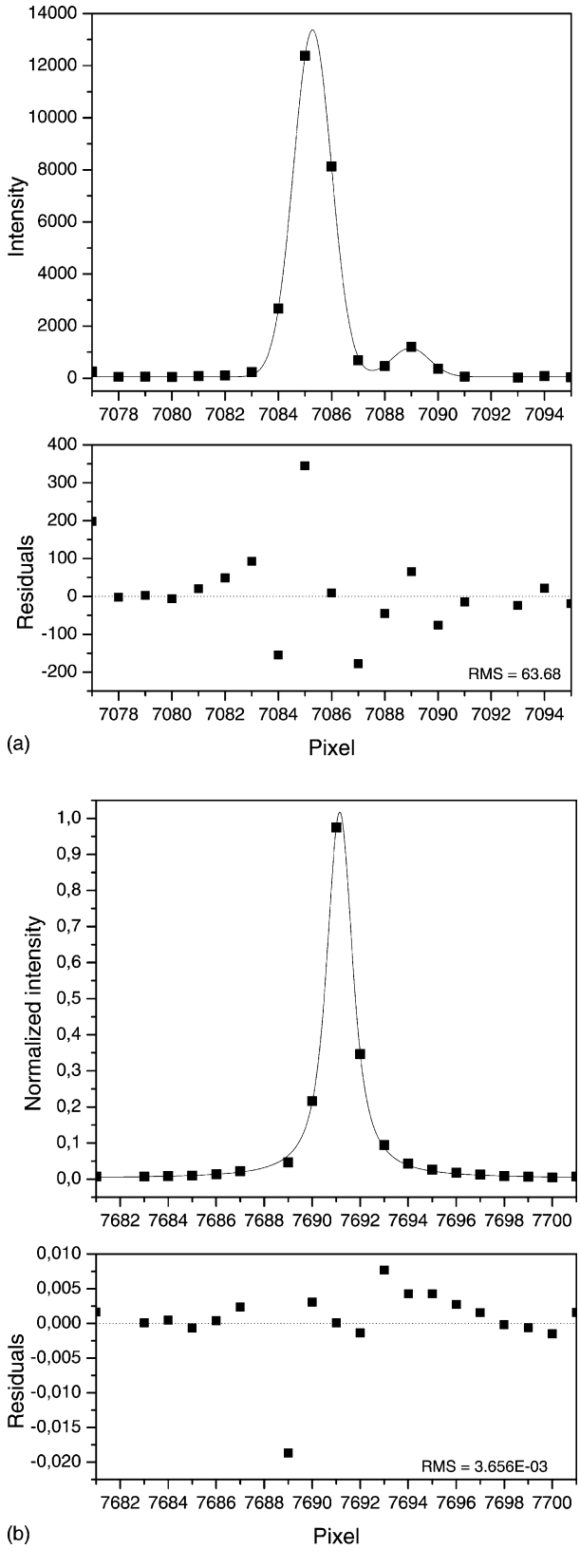

Fig. 13. Instrumental line shape of SCIAMACHY in channels 7 and 8. (a) Spectral lines of the CrPtNe hollow cathode lamp in channel 7 fitted by a Gaussian function and according residuals of the fit. (b) Spectral line of the CrPtNe hollow cathode lamp in channel 8 fitted by a Voigt profile and according residuals of the fit.

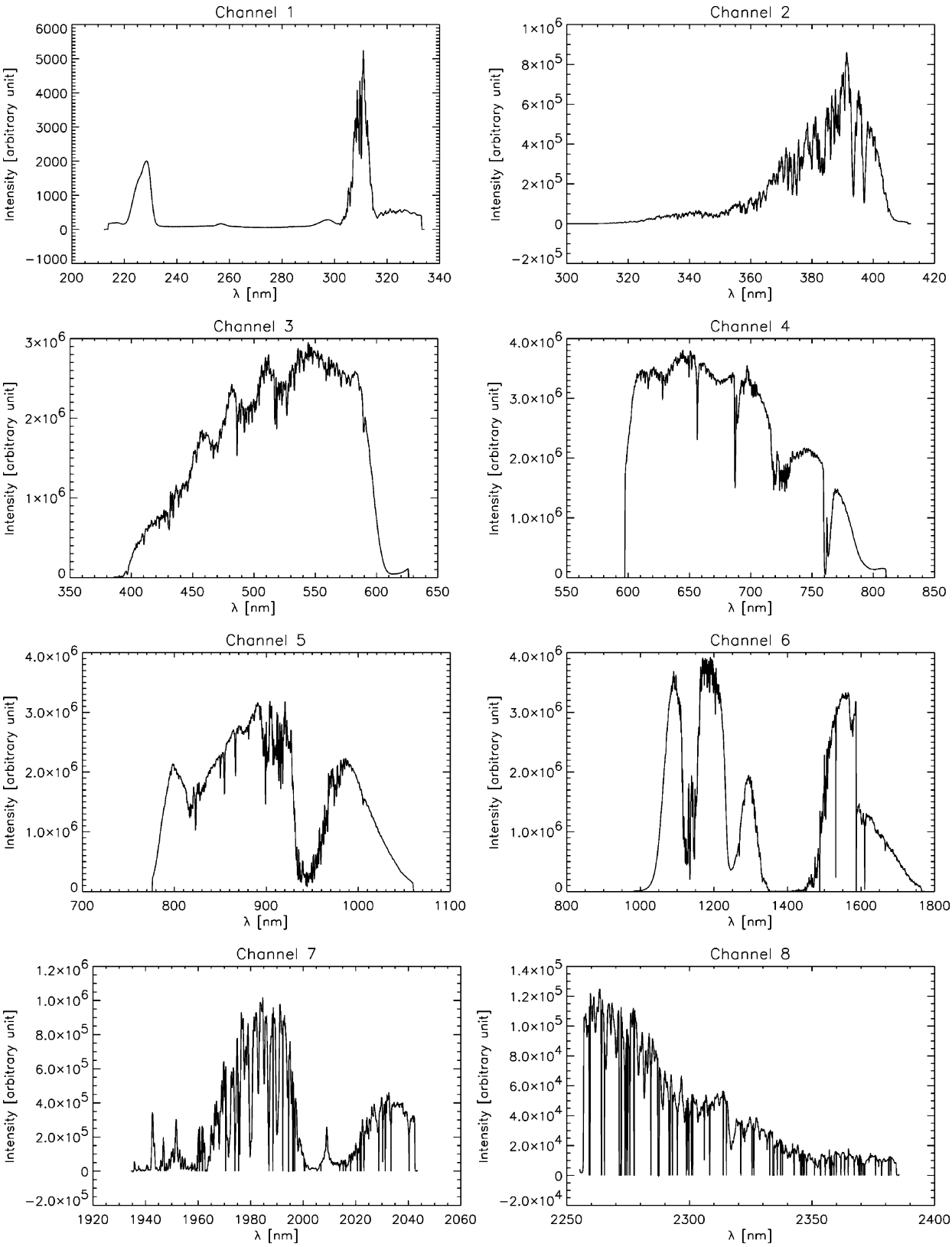

Fig. 14. Solar occultation spectrum measured with SCIAMACHY on-ground. Note the straylight features in channel 1 (see text for discussion). The spectra were not corrected for “hot” and “bad” pixels in the infrared channels.

and in the entire channel 7, strong lines useful for spectral calibration are missing and the polynomial expressions for transformation of pixel numbers into wavelengths have to be extrapolated. Therefore, molecular absorption structures were used for improving the wavelength calibration in these regions (see Fig. 12b). To determine the pixel positions of the molecular structures, the optical density spectra as a function of the pixel numbers were interpolated on a finer wavelength grid. The centre wavelengths of the molecular absorption structures were determined using calibrated molecular spectra measured by Fourier-transform spectroscopy at the same temperatures [7,10,13] and convoluted with the SCIAMACHY ILS provided by industry. A fifth-order polynomial was fitted to the data using a linear least-squares fit. The residuals are smaller than 0.01 nm in the middle of the channels and slightly larger at the borders of the channels.

7.2. Instrumental line shape

The SCIAMACHY instrumental line shape (ILS) is a function of wavelength that needs to be determined for each channel by fitting different functions to the spectral lines of a CrPtNe hollow cathode lamp. For channels 1–6, the type of the ILS function (simple hyperbolic function for channels 1–5 and a Gaussian function for channel 6) and its FWHM for each channel were provided by industry [3], see Table 1.

In this study, highly resolved molecular spectra measured by Fourier-transform spectroscopy [7,9,10,13,25] were convoluted with the ILS function (assuming that a constant FWHM for each channel) and compared to the spectra measured with the SCIAMACHY spectrometer. The agreement was generally good, except for channel 1. In this channel the convolution with the same ILS function but with a smaller FWHM resulted in a better agreement.

The ILS function in the channels 7 and 8 was derived from measurements performed during the "Delta-PI-period" after realignment of the diode-array detectors ("shimming") by industry, see also Figs. 6 and 7. Different analytical functions were fitted to the spectral lines of the CrPtNe lamp using a non-linear least-squares fitting routine. From these fits the type of the ILS function in the near-IR channels was determined (see as example, Fig. 13). The ILS function in channel 7 is best reproduced by a Gaussian function (FWHM 1.7 pixels) and in channel 8 by a Voigt function (FWHM 1.3 pixels). Because there are only a few spectral lines in each channel, the wavelength dependence of the FWHM of the ILS function could not be determined. However, for this purpose, molecular absorption spectra can provide the necessary information because some of them show bands of regularly spaced lines over the entire channels. As mentioned above, molecular absorption spectra (CO, CO_2, CH_4, H_2O, N_2O) were measured at a total pressure of 500 mbar using N_2 as buffer gas in order to broaden the spectral lines and to prevent their saturation. Using these spectra for characterizing the ILS the pressure broadening has to be taken into account. The FWHM of the pressure broadened lines is between 0.2 and 0.4 pixels (0.02 and 0.06 nm), respectively. Because of the pressure broadening (the total pressure was 500 mbar to avoid saturation problems) the molecular lines in channel 7 also were fitted using a Voigt profile because the convolution of the Lorentzian line shape of a pressure broadened molecular line with the Gaussian slit function is a Voigt profile. The Doppler line width is negligibly small compared to the pressure broadening under these conditions.

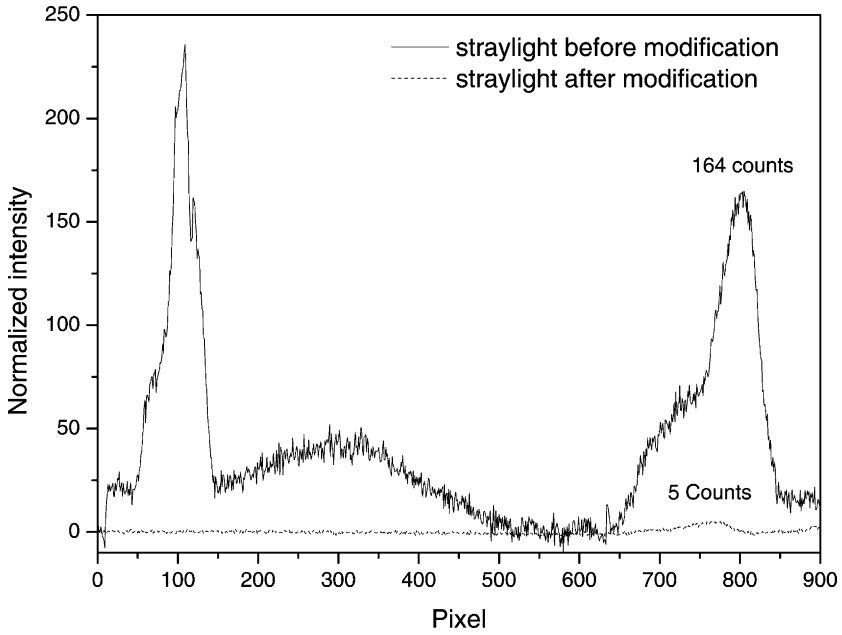

Fig. 15. Straylight characterization in the UV. Straylight before and after the modification of SCIAMACHY channel 1 (using O_3 as filter).

7.3. Straylight properties

Especially in the ultraviolet wavelength region, a high suppression of straylight in the satellite spectrometer is essential because the solar radiance varies over about two orders of magnitude in the wavelength region 200–350 nm, and the earthshine radiance even over approximately four orders of magnitude. At the same time, it is rather difficult to obtain an accurate correction for straylight in such complex instruments like SCIAMACHY and GOME [32]. Generally, to investigate the straylight properties of the instruments, narrow-band spectral filters or stimuli are used by industry. However, it should be pointed out that molecular absorbers at appropriate partial pressures are also very good filters in some wavelength regions. In particular, a small amount of ozone in the cell absorbs extremely well all light in the ultraviolet wavelength region by the strong absorption of the Hartley band but lets pass all the light in other wavelength regions (above ca. 320 nm). For instance, one can clearly identify strong parasitic straylight in ground-based solar occultation spectra measured with SCIAMACHY (Fig. 14) in channel 1. This observation actually led to another refurbishment of the SCIAMACHY instrument in late 1999 in order to reduce the straylight in channel 1. The trace gas measurements that have been performed to quantify the straylight in the UV using gaseous O_3 as filter clearly show the improvement: after the refurbishment of the SCIAMACHY channel 1 (230–314 nm) the straylight was reduced by a factor of 30 (Fig. 15).

8. Conclusions

In this paper, measurements of trace gas absorption spectra using the SCIAMACHY PFM satellite instrument have been presented. The absorption spectra have been measured at medium spectral resolution over a broad spectral range and at temperatures between 203 and 293 K. They show high signal-to-noise ratio (up to several 10^3), high baseline stability (less than 1% variation) and an accurate wavelength calibration (better than 0.01 nm). For O_3, NO_2 (including the first measurement at 203 K) and SO_2 (with new spectra at temperatures down to 203 K which might become interesting in the future for limb-scanning measurements of stratospheric SO_2 after volcanic eruptions) a temperature parametrization is used to model the absorption cross-sections. With this parametrization the absorption cross-sections in certain wavelength regions can be calculated at intermediate temperatures with an error smaller than 2%. The absorption cross-sections were successfully used to improve the wavelength calibration of the SCIAMACHY spectrometer and to characterize the ILS function and the straylight properties of the instrument.

In conclusion, the measurement of molecular trace gas absorption spectra prior to launch is an important tool for instrument characterization and for improving the spectroscopic database, together with laboratory work providing spectra at high-resolution, i.e. with an ILS narrower than the smallest widths of the molecular absorption structures [33].

All data presented in this paper are available in digital form by request to any of the authors, or on the WWW (http://www.iup.physik.uni-bremen.de/gruppen/molspec/).

Acknowledgements

This project has been supported by the German Space Agency (DLR-Bonn, formerly DARA) under grants No. 50EP9207 and 50EE9931 and by the University and Land of Bremen. The authors wish to thank the many scientists and engineers at SRON (in particular A. Goede (now at KNMI), R. Snels, M. Dobber, R. van der Linden), at TPD/TNO (in particular C. Olij, M. Te Plate, E. Zoutman), at Fokker Space and Systems (T. Watts, A. Kamp, T. van den Meer) and at Dornier-Astrium (W. Fricke, P. Lützow-Wentzky and the EGSE-operators), and Jörg Callies, Chris Readings and Tobias Wehr from ESA-ESTEC for their important support during the “PI-”, the “Delta PI-” and the “Delta2-PI-Periods”. We want to apologize that not all people who have contributed to this study might have been mentioned here.

References

[1] J.B. Burrows, E. Hölzle, A.P.H. Goede, H. Visser, W. Fricke, SCIAMACHY—scanning imaging absorption spectrometer for atmospheric chartography, Acta Astronaut. 35 (1995) 445–451.
[2] H. Bovensmann, J.P. Burrows, M. Buchwitz, J. Frerick, S. Noël, V.V. Rozanov, SCIAMACHY: mission objectives and measurements modes, J. Atmos. Sci. 56 (1999) 127–150.
[3] SCIAMACHY PFM calibration results review data package, TPD-TNO, Delft, 1999.
[4] J.U. White, Long optical paths of large aperture, J. Opt. Soc. Am 32 (1942) 285–288.
[5] R. Snel, personal communication, 1998.
[6] M.H. Harwood, R.L. Jones, Temperature dependent ultraviolet-visible absorption cross sections of NO_2 and N_2O_4: low-temperature measurements of the equilibrium constant of $2NO_2 \leftrightarrow N_2O_4$, J. Geophys. Res. D 99 (1994) 22955–22964.
[7] S. Voigt, Hochauflösende Fourier-Transform-Spektroskopie atmosphärischer Spurengase im ultravioletten, sichtbaren und nahinfraroten Spektralbereich: CO, NO_2 und O_3, Ph.D. Thesis, University of Bremen, 1998.
[8] A.M. Bass, R.J. Paur, The ultraviolet cross-sections of Ozone: I. The measurements II. Results and temperature dependence, in: C. Zerefos, A. Ghazi (Eds.), Proceedings of the Quadrennial Ozone Symposium on Atmospheric Ozone, Halkidiki, Greece, Reidel, Dordrecht, 1985, pp. 606–616.
[9] A.C. Vandaele, C. Hermans, P.C. Simon, M. Carleer, R. Colin, S. Fally, M.F. Merienne, A. Jenouvrier, B. Coquart, Measurements of the NO_2 absorption cross-section from 42000 to 10000 cm^{-1} (238–1000 nm) at 220 and 294 K, J. Quant. Spectrosc. Radiat. Transfer 59 (1998) 171–184.

[10] A.C. Vandaele, P.C. Simon, J.M. Guilmot, M. Carleer, R. Colin, SO_2 absorption cross section measurement in the UV using a Fourier transform spectrometer, J. Geophys. Res. 99 (1994) 25599–25605.
[11] J.P. Burrows, A. Richter, A. Dehn, B. Deters, S. Himmelmann, S. Voigt, J. Orphal, Atmospheric remote-sensing reference data from GOME—2. Temperature-dependent absorption cross sections of O_3 in the 231–794 nm range, J. Quant. Spectrosc. Radiat. Transfer 61 (1999) 509–517.
[12] J. Orphal, A critical review of the absorption cross sections of O_3 and NO_2 in the 240–790 nm region, ESA Technical Note MO-TN-ESA-GO-0302, ESA Earth Observation Programmes Development Department, ESTEC Noordwijk, 2002.
[13] H. Kromminga, J. Orphal, P. Spietz, S. Voigt, J.P. Burrows, The temperature dependence (213–293 K) of the absorption cross sections of OClO in the 340–450 nm region measured by Fourier-transform spectroscopy, J. Photochem. Photobiol. A, this issue.
[14] L.S. Rothman, C.P. Rinsland, A. Goldman, S.T. Massie, D.P. Edwards, J.-M. Flaud, A. Perrin, C. Camy-Peyret, V. Dana, J.-Y. Mandin, J. Schroeder, A. McCann, R.R. Gamache, R.B. Wattson, K. Yoshino, K.V. Chance, K.W. Jucks, L.R. Brown, V. Nemtchinov, P. Varanasi, The HITRAN molecular spectroscopic database and HAWKS (HITRAN atmospheric workstation) 1996 edition, J. Quant. Spectrosc. Radiat. Transfer 60 (1998) 665–710.
[15] K. Bogumil, Absorptionsspektroskopische Messungen von atmosphärischen Spurengasen im ultravioletten, sichtbaren und nah-infraroten Spektralbereich mit dem SCIAMACHY Pre-Flight Model, Ph.D. Thesis, University of Bremen, 2003.
[16] R. Bacis, A.J. Bouvier, J.F. Flaud, The ozone molecule: electronic spectroscopy, Spectrochim. Acta A 54 (1988) 17–34.
[17] A. Barbe, S. Bouazza, J.J. Plateaux, M. Jacon, The $3\nu_3 + 2\nu_2$ band of ozone: line positions and intensities, J. Mol. Spectrosc. 162 (1993) 335–341.
[18] A. Barbe, O. Sulakshina, J.J. Plateaux, Vl.G. Tyuterev, S. Bouazza, Line positions and intensities of the $3\nu_1 + \nu_3$ band of ozone, J. Mol. Spectrosc. 175 (1996) 296–302.
[19] J.M. Flaud, A. Barbe, C. Camy-Peyret, J.J. Plateaux, High resolution analysis of the $5\nu_3$, $3\nu_1 + \nu_2 + \nu_3$, and $\nu_1 + 4\nu_3$ band of $^{16}O_3$: line positions and intensities, J. Mol. Spectrosc. 177 (1996) 34–39.
[20] A. Barbe, J.J. Plateaux, Vl.G. Tyuterev, S. Mikhailenko, Analysis of high resolution measurements of the $2\nu_1 + 3\nu_3$ band of ozone: coriolis interaction with the $\nu_1 + 3\nu_2 + 2\nu_3$ band, J. Quant. Spectrosc. Radiat. Transfer 59 (1998) 185–194.
[21] A. Barbe, A. Chichery, The $2\nu_1 + \nu_2 + 3\nu_3$ band of $^{16}O_3$: line positions and intensities, J. Mol. Spectrosc. 192 (1998) 102–110.
[22] L.T. Molina, M.J. Molina, Absolute absorption cross sections of ozone in the 185 to 350 nm wavelength range, J. Geophys. Res. 91 (1986) 14501–14508.
[23] J.B. Burkholder, R.K. Talukdar, Temperature dependence of the ozone absorption spectrum over the wavelength range 410–760 nm, Geophys. Res. Lett 21 (1994) 581–584.
[24] J. Brion, A. Chakir, J. Charbonnier, D. Daumont, C. Parisse, J. Malicet, Absorption spectra measurements for the ozone molecule in the 350–830 nm region, J. Atmos. Chem. 30 (1998) 291–299.
[25] S. Voigt, J. Orphal, K. Bogumil, J.P. Burrows, The temperature dependence (203–293 K) of the absorption cross sections of O_3 in the 230–850 nm region measured by Fourier-transform spectroscopy, J. Photochem. Photobiol. A 143 (2001) 1–9.
[26] T.P. Kurosu, K.V. Chance, T. Yokota, Y. Sasano, Polar stratospheric cloud detection from the ILAS instrument, in: Y. Sasano, J. Wang, T. Hayasaka (Eds.), Proceedings of SPIE on Optical Remote Sensing of the Atmosphere and Clouds vol. II, vol. 4150, 2001, pp. 68–75.
[27] J.P. Burrows, A. Dehn, B. Deters, S. Himmelmann, A. Richter, S. Voigt, J. Orphal, Atmospheric remote sensing reference data from GOME: Part 1. Temperature-dependent absorption cross sections of NO_2 in the 231–794 nm range, J. Quant. Spectrosc. Radiat. Transfer 60 (1998) 1025–1031.
[28] C.H. Hearn, J.A. Joens, The near UV absorption spectrum of CS_2 and SO_2 at 300 K, J. Quant. Spectrosc. Radiat. Transfer 45 (1991) 69–75.
[29] A. Wahner, G.S. Tyndall, A.R. Ravishankara, Absorption cross sections for OClO as a function of temperature in the wavelength range 240–480 nm, J. Phys. Chem. 91 (1987) 2734–2738.
[30] J.E. Murray, Atlas of the spectrum of a platinum/chromium/neon hollow-cathode reference lamp in the region 240–790 nm, Final Report, Imperial College, London, 1995.
[31] J. Orphal, S. Voigt, J.P. Burrows, High-resolution Fourier-transform spectra of a Pt/Cr-Ne hollow-cathode emission lamp between 780 and 2500 nm, Final Report, University of Bremen, 1997.
[32] R.M. Koopman, in: Proceedings of the 3rd ERS Symposium on Analysis of GOME Straylight, ESA SP-414, vol. 2, 1998, pp. 733–737.
[33] J. Orphal, K. Bogumil, A. Dehn, B. Deters, S. Dreher, O.C. Fleischmann, M. Hartmann, S. Himmelmann, T. Homann, H. Kromminga, P. Spietz, A. Türk, A. Vogel, S. Voigt, J.P. Burrows, Laboratory spectroscopy in support of UV-Visible remote-sensing of the atmosphere, in: Recent Research Developments in Physical Chemistry, vol. 6, Transworld Research Network, Trivandrum, 2002, pp. 15–34.